Environmental Science & Technology

pubs.acs.org/est

Article

Characterizing Operating Condition-Based Formaldehyde Emissions of Light-Duty Diesel Trucks in China Using a PEMS-HCHO System

Manni Zhu, Jiamin Ou, Songdi Liao, Fei Yu, Menghua Lu, Qinge Sha, Junwen Liu, Hancheng Zhong, Zeyan Wu, Zhuangmin Zhong, and Junyu Zheng*

Cite This: *Environ. Sci. Technol.* 2023, 57, 1592−1599

Read Online

ACCESS | Metrics & More | Article Recommendations | Supporting Information

ABSTRACT: Formaldehyde (HCHO) plays a critical role in atmospheric photochemistry and public health. While existing studies have suggested that vehicular exhaust is an important source of HCHO, the operating condition-based diesel truck HCHO emission measurements remain severely limited due to the limited temporal resolution and accuracy of measurement techniques. In this study, we characterized the second-by-second HCHO emissions from 29 light-duty diesel trucks (LDDTs) in China over dynamometer and real-world driving tests using a portable online HCHO emission measurement system (PEMS-HCHO), considering various operating conditions. Our results suggested that the HCHO emissions from LDDTs might be underestimated by the widely used offline DNPH-HPLC method. The HCHO emissions at a 200 s cold start from China V LDDT can be up to 50 mg/start. Different driving conditions over dynamometer and real-world driving tests led to a 2−4 times difference in the HCHO emission factors (EFs). Under real-world hot-running conditions, the HCHO EFs of China III, IV, V, and VI LDDTs were 43.5 ± 35.7, 10.6 ± 14.2, 8.8 ± 5.1, and 3.2 ± 1.2 mg/km, respectively, which significantly exceeded the latest California low emission vehicle III HCHO emission standard (2.5 mg/km). These findings highlighted the significant impact of vehicle operating conditions on HCHO emissions and the urgency of regulating HCHO emissions from LDDTs in China.

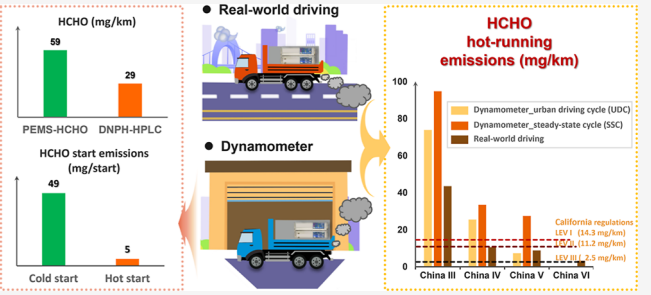

KEYWORDS: *formaldehyde, light-duty diesel trucks, vehicle operating conditions, dynamometer tests, real-world driving emissions tests, online emission measurement*

1. INTRODUCTION

Formaldehyde (HCHO) in the atmosphere is a highly active species that is responsible for tropospheric secondary pollution, and it imposes severe threat to human health as one of the most detrimental hazardous air pollutants.[1−4] HCHO can be directly emitted from various natural and anthropogenic sources (primary HCHO), and it can be produced from the photooxidation of hydrocarbons (secondary HCHO).[5,6] Although secondary HCHO is the largest contributor to total atmospheric HCHO,[7] primary HCHO is an important contributor to ambient HCHO and ozone (O_3) formation.[5,8,9] However, field observations have indicated that the modeling simulations have greatly underestimated HCHO concentrations by 45%, most likely due to the missing sources of primary HCHO.[10] Studies in China and Mexico suggested that emission inventories might underestimate the HCHO emissions from primary anthropogenic sources by two to three times, as suggested by ambient measurement[11] and on-road measurement.[12] A better understanding and characterization of the primary HCHO emission sources are in need.

Vehicle exhaust is an important primary source of atmospheric HCHO.[13,14] In many countries, the HCHO emissions from vehicles are regulated. For decades, the USA has set and strengthened the HCHO emission standards of vehicles in tier and low emission vehicle (LEV) regulations. Additionally, Brazil and Korea have had vehicular HCHO emission standards for many years. Europe is considering to include HCHO as a regulated pollutant in the Euro VII emission standards. However, there is no HCHO emission standard for vehicles in China, partly due to a lack of understanding on the HCHO emission characteristics of vehicles. Although light-duty passenger cars have been reported to have near-zero HCHO emissions due to the implementation of the newest Euro VI and China VI standards,[15−17] diesel trucks have been found to emit high levels of HCHO.[18,19] However, to the best of our knowledge, there are only a few studies on HCHO emissions from diesel

Received: October 20, 2022
Revised: January 11, 2023
Accepted: January 11, 2023
Published: January 20, 2023

trucks in China,[19−22] all of which have used offline 2,4-dinitrophenylhydrazine (DNPH) cartridges with chromatography analysis to determine HCHO emissions. This DNPH method is likely to induce large biases for HCHO quantification due to its sampling efficiency, interference from NO_x, and the measurement accuracy under high temperature, humidity, and NO_x emissions.[23−25] In addition, the DNPH method cannot be used to characterize HCHO emissions with high temporal resolution. Though several studies have employed online Fourier transform infrared spectroscopy and proton-transfer reaction mass spectrometry to measure HCHO from vehicles,[26−29] problems of limited measurement range, large equipment size, and high demand of energy consumption to support on-road testing remain outstanding. Therefore, there are large gaps in our understanding of the HCHO emissions from diesel trucks and the impacts of their operating conditions on HCHO emissions.

To better understand HCHO emissions from diesel trucks, in this study, we investigated HCHO emissions of 29 light-duty diesel trucks (LDDTs) under different operating conditions using a self-developed online portable emission measurement system for HCHO (PEMS-HCHO).[30] Based on the online measurements, we quantified the second-by-second HCHO emission characteristics and discussed the impacts of the operating conditions on the HCHO emissions. Additionally, the HCHO emission factors (EFs) of LDDTs under different operating conditions were established. The findings of this study provide a better quantification of HCHO emissions from diesel trucks and scientific evidence for LDDT HCHO emission regulation in China.

2. MATERIALS AND METHODS

2.1. Vehicle Information. In this study, a total of 29 LDDTs were measured. Among these vehicles, 15 LDDTs were tested with dynamometer experiments, 12 LDDTs were tested under real-world driving conditions, and 2 LDDTs were tested with both the dynamometer and real-world driving tests. The LDDTs were randomly recruited from car rental agencies in Guangzhou. These LDDTs were compliant with China III, IV, V, and VI standards, which are representative considering their share in the diesel truck population of China.[31] The engines and fuels of LDDTs are regulated by the emission standard and fuel quality standard, respectively. For most LDDTs comply with China III standard, they are equipped with four-cylinder high-pressure direct injection engines. The China IV−China VI LDDTs mainly have four-cylinder high-pressure common rail fuel injection engines. Under the sixth-phase fuel quality standards of China, all the LDDTs use the commercial 0# diesel (without biodiesel blends) in Guangzhou. For the LDDTs we used for the experiment, they cover the above engine types and fuel. Model year of the tested LDDTs cover the years from 2009 to 2020, with weights ranging from 2160 to 2805 kg. Specifications of the LDDTs are provided in Tables S1 and S2. We tested 35 light-duty gasoline vehicles (LDGVs) (passenger cars) compliant from China I to China VI over the dynamometer for comparison; specifications of the LDGVs are detailed in Table S3.

2.2. Measurement Devices. Highly temporally resolved (second-by-second) HCHO concentrations and the corresponding vehicle activities were measured by the online PEMS-HCHO, which can be used for both the dynamometer tests and the real-world driving emission (RDE) tests. The PEMS-HCHO includes a pretreatment module, an auxiliary parameter measurement module, and a portable online HCHO measurement instrument (Hantzsch-Abs), as introduced and demonstrated in our previous study.[30] Tailpipe emissions were first sampled using the portable pretreatment module before entering the Hantzsch-Abs to prevent the loss of HCHO from the high temperature and humidity and to provide high dilution ratios for the exhausts. This pretreatment module was based on split-flow dilution method and used high-pure nitrogen as dilution gas. The uncertainty of the dilution ratio was reported to be ±5%, with more details of the pretreatment module in a study by Liao *et al.*[32] The Hantzsch-Abs was based on the Hantzsch reaction and absorption photometry, and it featured the application of liquid waveguide capillary cells to achieve high detection sensitivity and online measurements for HCHO. In this study, we adjusted the measurement range to be 0−1.8 ppmv, and the limit of detection was 0.04 ppbv. The auxiliary parameter measurement module included an on-board diagnostics system, a global positioning system, and a slope meter to collect real-time engine and vehicle activity data, such as engine speed, vehicle speed, and road slope. Details of the field deployments can be seen in the Supporting Information.

In addition, we used a SEMTECH EFM-2 flowmeter to obtain the exhaust flow rate, temperature, and relative humidity. To verify the dilution ratio, CO_2 concentrations in the raw exhausts were detected by a SEMTECH-DS (Sensors, Inc., USA); then, the concentrations were compared to the diluted CO_2 concentrations provided using a CO_2 analyzer (Li-840A. Licor, Inc.) connected to the pretreatment module. All the measurement devices had the same data acquisition frequency at 1 Hz, and all the data were synchronized on a second-by-second basis. To ensure the accuracy of the test results, the measurement devices were zeroed before and after each test and calibrated with standard gases/solutions before the first test of each day.

2.3. Test Cycles over the Dynamometer. Two testing cycles widely used were adopted for LDDTs during the dynamometer tests: urban driving cycle (UDC) and steady-state cycle (SSC) (see Figure S5). The UDC is composed of four repeated Economic Commission for Europe (ECE) cycles without interruption. An ECE cycle lasts for 195 s with an accumulated distance of 1.13 km. The SSC consists of three different constant speed stages of 20, 40, and 60 km/h, each lasting for 4 min. All LDDTs were measured by hot-start cycles, while two of the China V LDDTs (coded D12 and D13) were tested by cold-start UDC to investigate the impacts of start modes. Emission measurements under cold-start conditions were performed by soaking the vehicles for at least 6 h at a test temperature of 20−30 °C; hot-start conditions were obtained by warming the vehicles fully and then turning them off for 10 min.

2.4. Driving Route for Real-World Driving Emission Tests. To investigate the discrepancies between laboratory dynamometers and real-world roads, 14 LDDTs were tested on open roads in the Panyu district of Guangzhou city, which comprised ∼40% suburban roads (non-highway phase) and ∼60% highways, as shown in Figure S6. This test route covered the representative driving road types for LDDTs in Guangzhou. Basic information about the route is shown in Table S4. The lengths of the test routes ranged from 55 to 58 km, and the road slope ranged from −5.34 to 3.60%. Each vehicle was measured for two to three trips over the same route, both clockwise and counterclockwise. All vehicles were

https://doi.org/10.1021/acs.est.2c07744
Environ. Sci. Technol. 2023, 57, 1592−1599

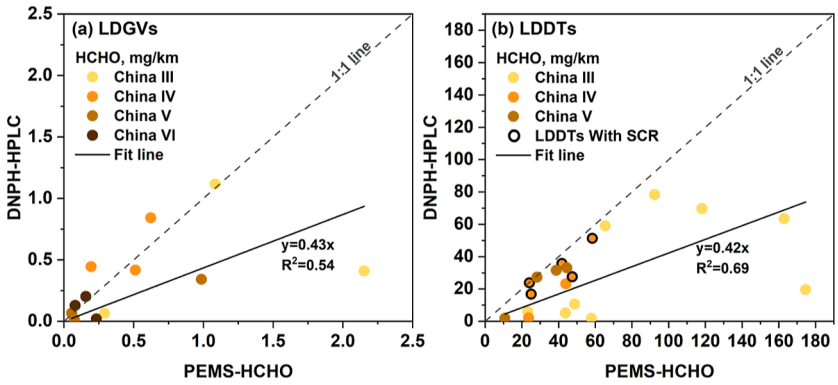

Figure 1. Scatter plots of the HCHO EFs measured by the PEMS-HCHO and the DNPH-HPLC for (a) LDGVs and (b) LDDTs. In the right panel, the dot points with solid border represent the results of the LDDTs with SCR devices, and the dots without border indicate the results of LDDTs without SCR.

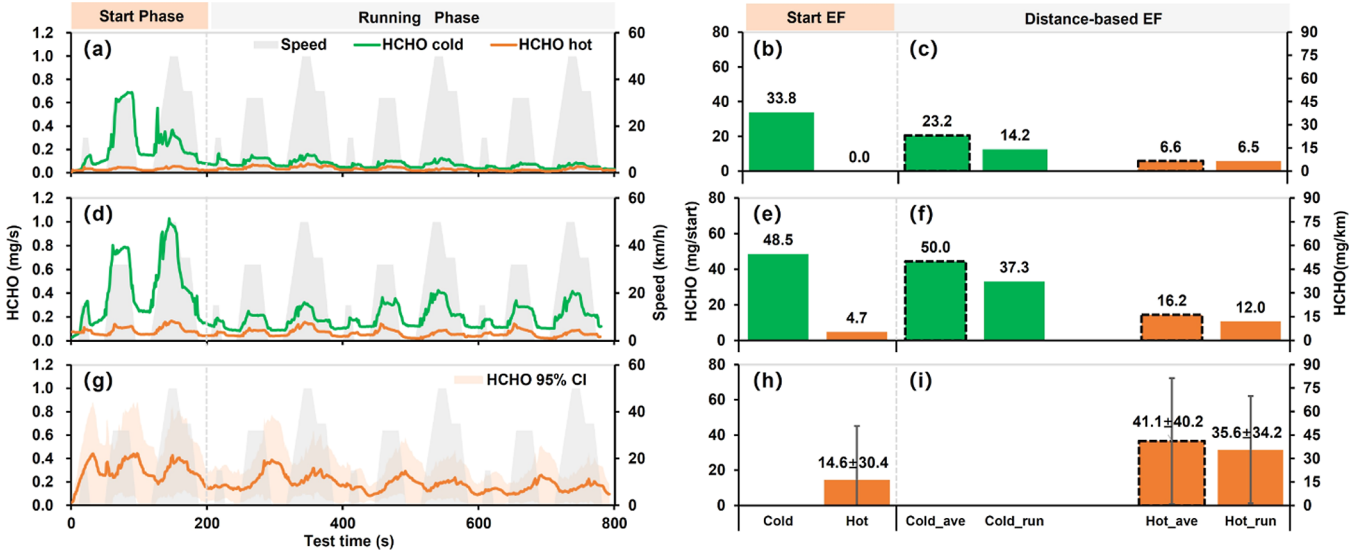

Figure 2. (a) Second-by-second HCHO emission rates, (b) start EFs, and (c) comparison of the total average EFs (dashed box) and running EFs for the D12 China V LDDT under cold-start (green) and hot-start (orange) UDC testing; (d–f) for the D13 China V LDDT; and (g–i) for all LDDTs tested at the hot-start mode, of which the solid line represents average values from all the test vehicles, and the shaded areas represent 5 and 95% confidence intervals for the second-by-second emission profile.

tested after being fully warmed up to maintain hot-running conditions throughout testing.

3. RESULTS AND DISCUSSION

3.1. Comparisons of HCHO Emissions between PEMS-HCHO and DNPH-HPLC. Previous experiments usually used the DNPH sampling with the high-performance liquid chromatography analysis (DNPH-HPLC) method to detect HCHO emissions, which was suspected to underestimate HCHO in a diesel engine-operated environment.[22] In this study, we conducted a comparison experiment between the PEMS-HCHO and DNPH-HPLC methods over the dynamometer test to investigate the discrepancy between the two methods. In total, 12 samples of LDGVs and 20 samples of LDDTs were measured by both the PEMS-HCHO and DNPH-HPLC.

As shown in Figure 1a, the HCHO EFs for LDGVs measured by the PEMS-HCHO *versus* the DNPH-HPLC were highly concentrated around the diagonal line (the 1:1 line, as shown in Figure 1a). It suggests that the results detected by the two methods were consistent. Also, the HCHO EFs of LDGVs in this study were close to the results from other studies (see Table S5). These results suggested that the PEMS-HCHO system was reliable for the exhaust HCHO emission measurements.

As shown in Figure 1b, the HCHO emissions from LDDTs were approximately 2 orders of magnitude higher than those of LDGVs. In addition, most of the HCHO EFs determined by the DNPH-HPLC were obviously lower than the results measured by the PEMS-HCHO. To further evaluate the reliability of PEMS-HCHO, we conducted comparison tests between the Hantzsch-Abs in the PEMS-HCHO and a commercial online HCHO measurement instrument (the Hantzsch-flu, formaldehyde-monitor AL4021, Aero-Laser) over the dynamometer (see Text S2). Results from the Hantzsch-Abs at the high HCHO emission level were slightly lower than the Hantzsch-flu. The observed differences might be attributed to the lower sampling efficiency of the Hantzsch-Abs and higher interferences from other carbonyls in the Hantzsch-flu. Overall, these two instruments showed a good agreement, indicating that the PEMS-HCHO was also reliable for HCHO measurements at high emission conditions.

https://doi.org/10.1021/acs.est.2c07744
Environ. Sci. Technol. 2023, 57, 1592−1599

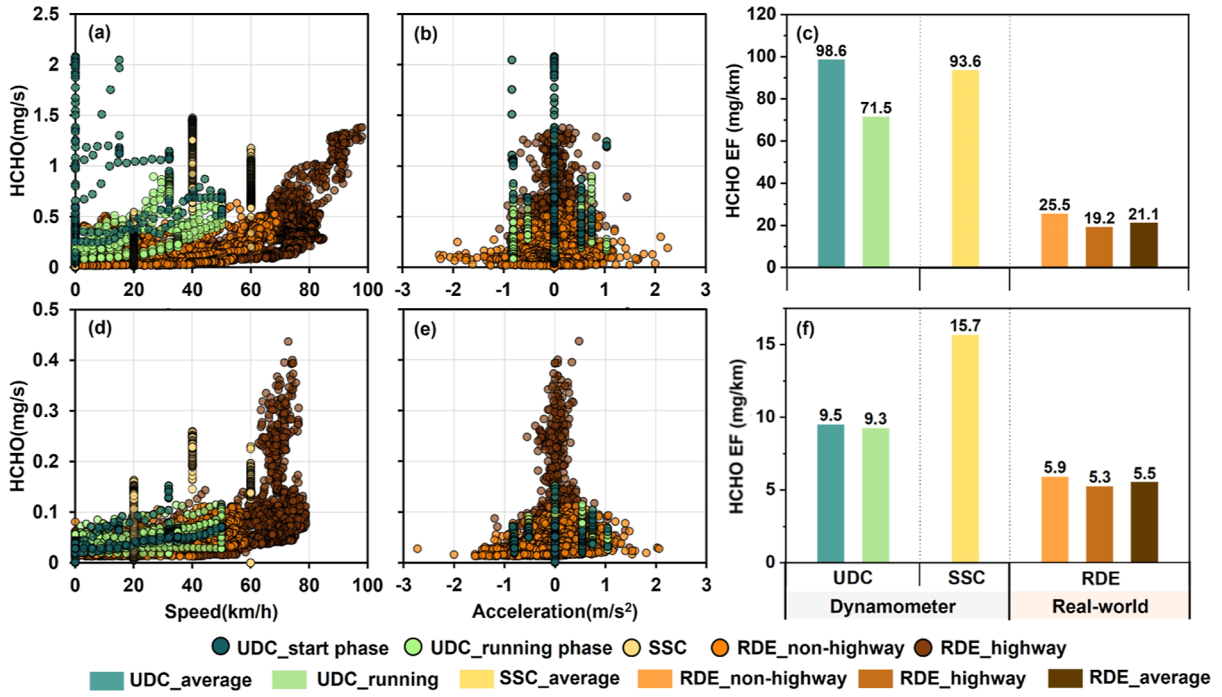

Figure 3. (a) HCHO emission rates as a function of vehicle speeds, (b) HCHO emission rates as a function of accelerations, and (c) HCHO EFs comparison during UDC, SSC, and RDE testing for the D2 China III (also the R4) LDDT; and (d–f) for the D8 (also the R5) China IV LDDT.

Therefore, the differences between PEMS-HCHO and DNPH-HPLC for LDDTs might be attributed to the fact that: (a) the DNPH cartridges cannot completely capture HCHO due to limited sampling volume of cartridge and high carbonyl emissions by LDDTs;[19] (b) high NO_x and CO emissions in LDDT exhausts could consume the DNPH cartridges, which lead to the loss of HCHO;[23] and (c) high temperature and humidity in LDDT exhausts could result in HCHO loss for directly sampling without pretreatment. These factors affected the HCHO measurement accuracy of the DNPH-HPLC for LDDTs. However, for the LDGVs, these factors had less impacts on the DNPH-HPLC measurements due to the lower HCHO, NO_x and CO emissions, and exhausts temperatures (see Texts S6 and S10). As a result, measurements between two methods were more consistent. Similarly, discrepancies of the measurement results for the LDDTs with selective catalytic reduction (SCR) devices were relatively smaller, as shown in Figure 1b, given the lower NO_x emissions from the LDDTs with SCR (see Text S11) and thus less interferences on the DNPH-HPLC measurements.

The above results showed that the DNPH-HPLC method might underestimate HCHO emissions from LDDTs, while the PEMS-HCHO is a more reliable method for measuring HCHO emissions from LDDTs. Therefore, the following analyses will be based on the measurement data by the PEMS-HCHO.

3.2. HCHO Start Emissions from the Dynamometer Test. Previous studies have demonstrated that vehicle starts have great influence on pollutant emissions such as volatile organic compounds and NO_x.[33,34] In this study, two LDDTs (coded as D12 and D13) were used to perform emission tests during the UDC under both cold- and hot-start modes to analyze the impacts of vehicle start modes on the HCHO emissions. The second-by-second HCHO emission rates (mass-based) are shown in Figure 2a,d. Extremely high HCHO emissions induced by the engine cold-start mode occurred within the initial 200 s for both vehicles. After that, the HCHO emissions dropped considerably. The proportions of HCHO emissions during the initial 200 s in the total cold-UDC emissions reached 53 and 44% for the D12 and D13 LDDTs, respectively (Figure S7). We investigated the effects of vehicle start modes on HCHO emissions from LDGVs and found that peak HCHO emissions occurred during the first 200 s in the cold-start mode, as shown in Text S6. The high emissions of HCHO under vehicle cold-start conditions were observed in other studies as well, but with varied occurrence periods ranging from 50 to 1000 s, probably due to different testing conditions.[26−28] In this study, we defined the duration of the initial 200 s after vehicle start as the start phase and the testing time after that as the running phase.

For the hot-start cycle, the HCHO emissions during the start phase were much lower than those during the cold-start cycle. While the HCHO emissions in the start phase did not increase significantly for D12 and D13 LDDTs, there were slight increase for the average HCHO emission of all LDDTs tested in the hot-start mode, as shown in Figure 2g. Ko *et al.* found there was no peak of HCHO emissions from diesel vehicles under idle conditions in the hot-start mode,[29] which might be explained by the low exhaust flows during idling. The high emissions during the start phase are relevant to the engine conditions. When the engine was recently ignited, the engine had not fully warmed up. As a result, the engine can produce much more HCHO due to the incomplete combustion of fuel in the vehicle engine, especially in the cold-start mode.[35]

Based on the second-by-second emission patterns, we quantified the start EFs (start EF in Figure 2) of the D12 and D13 LDDTs in both cold-start and hot-start modes, in addition to the average start EFs for all the LDDTs tested under hot-start UDC conditions. The start EFs were calculated from the increasing HCHO emissions during the start phase that were higher than the average emissions during the running phase according to the study of Wen *et al.*[33] (detailed are given

https://doi.org/10.1021/acs.est.2c07744
Environ. Sci. Technol. 2023, 57, 1592−1599

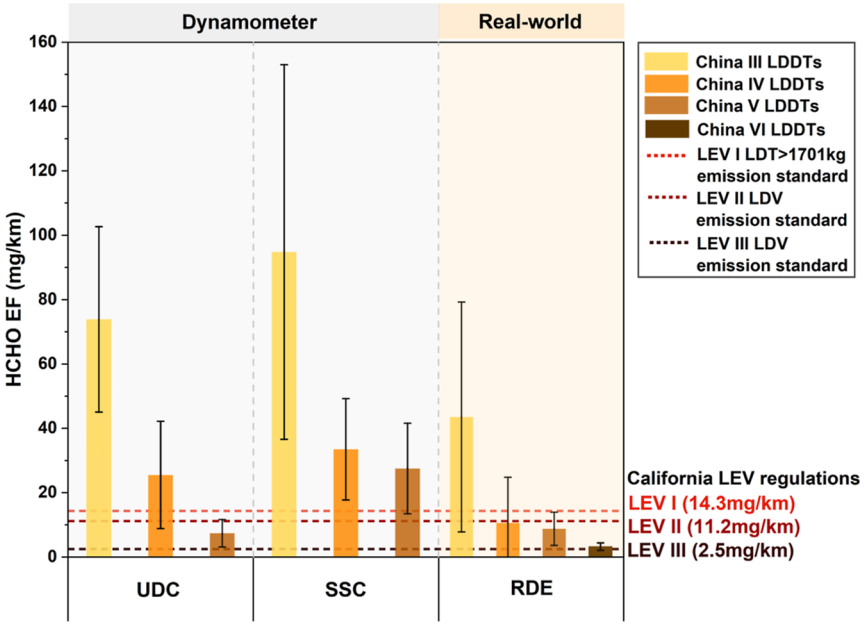

Figure 4. Hot-running HCHO EFs of LDDTs under UDC, SSC, and RDE tests; the columns and error bars are means and standard deviations, and the dashed lines represent the HCHO emission standards for LDT and LDV in LEV I−III regulations implemented by California.[48]

in Text S3). Additionally, we compared the running EFs of HCHO without increasing start emissions (the cold_run and hot_run distance-based EFs) and the total average EFs throughout testing (the cold_ave and hot_ave distance-based EFs) based on the test distances.

The cold-start EFs of HCHO for the D12 and D13 LDDTs were 33.8 and 48.5 mg/start, respectively, which were 10−14 times greater than those of gasoline vehicles (3.4 mg/start on average, see Figure S9). The ratio of the additional HCHO emissions from cold start to per-kilometer hot-running emissions (γ)[36] was 4−5 km for the two LDDTs. It is comparable to the ratios of CO and NO_x with 2−6 km of driving distance but much lower than HC and other volatile organic compounds such as benzene, toluene, and xylenes (ratios of 11−300 km).[33,34] After removing the effects of the increasing emissions from the cold-start phase, the running-phase EFs at the cold-start cycle were 39 and 25% smaller for the D12 and D13 LDDTs, respectively, compared to the total average EFs. For the hot-start mode, the increasing HCHO emissions for D12 were negligible and those for D13 LDDT were 4.7 mg/start, which were much smaller than the cold-start mode. On average, the hot-start HCHO EF was 14.6 ± 30.4 mg/start for all tested LDDTs. The hot-running EF decreased by 13% by excluding the additional emissions caused by hot start. These findings suggest that HCHO EFs can vary significantly from start modes and running conditions. The high HCHO emissions from cold-start also underline the necessity of targeted emission control.

3.3. Comparisons of HCHO Running Emissions between Dynamometer and RDE Tests. In addition to start modes, driving conditions during the running phase, such as vehicle speed and acceleration, are key factors affecting HCHO emissions. Discrepancies in HCHO emissions were observed by dynamometer tests based on various driving cycles.[15] In reality, a vehicle was operated under hot-running conditions with a warmed-up engine most of the time. It indicates that the running phase still make up an important contribution to HCHO emissions. In this study, the D2 LDDT (also coded R4) of the China III standard and the D8 LDDT (also coded R5) of the China IV standard were repeatedly tested under UDC, SSC, and RDE conditions (in the hot-start mode) to analyze the impacts of driving conditions on HCHO emissions.

Second-by-second HCHO emission profiles are shown in Figures S10 and S11, highlighting the fluctuations in mass-based HCHO emission rates and instantaneous fuel consumption. Figure 3 shows the transient HCHO emission rates *versus* speeds and accelerations, in addition to the distance-based HCHO EFs under different conditions. For UDC testing, the vehicle start effect on the increasing HCHO emissions was noticeable for the D2 LDDT. Notably, the distribution of HCHO emission rates during the running phase at the UDC condition varied from the non-highway phase during RDE testing (similar speed ranges). The running EFs of HCHO for UDC (71.5 mg/km for the D2 LDDT and 9.3 mg/km for the D8 LDDT) were higher than those of non-highway driving for RDE at the running phase (25.5 mg/km for the D2 LDDT and 5.9 mg/km for the D8 LDDT). Compared to the RDE non-highway phase, the UDC running phase consumes fuel much faster at a low speed and deceleration conditions (as shown in Figures S14−S16), which might contribute to the difference. In addition, compared to the RDE test, the higher fuel consumption under the SSC conditions led to higher HCHO emission rates and higher average EFs. These comparisons suggested that testing under the UDC and SSC driving conditions of dynamometers cannot reflect real-world emission characteristics.

Overall, the HCHO EFs derived from dynamometer tests were approximately 2−4 times higher than those from the RDE conditions. In other words, EFs generated from dynamometer tests would lead to significant overestimations of HCHO emissions from LDDTs.

3.4. HCHO Running Emissions from PEMS-HCHO. Based on the UDC, SSC, and RDE tests using the PEMS-HCHO, we developed the average hot-running HCHO EFs of LDDTs compliant with China III−VI standards, which are

https://doi.org/10.1021/acs.est.2c07744
Environ. Sci. Technol. 2023, 57, 1592−1599

presented in Figure 4. The measured HCHO EF for China III LDDTs was 73.9 ± 28.8 mg/km under UDC, excluding excess start emissions. This value was comparable to 94.8 ± 58.2 mg/km under SSC, while the HCHO EF derived from RDE tests was much lower (43.5 ± 35.7 mg/km). The relatively high HCHO emissions from the China III LDDTs were mainly attributed to the old direct injection engines, the higher accumulated mileages, and lack of aftertreatment devices. The RDE result was three times higher than that of a study on carbonyl emissions under hot-stable RDE testing in Beijing using the offline DNPH method,[19] with a calculated HCHO EF of 14.1 mg/km for China III LDDTs. The discrepancy is partly due to the slightly higher accumulated mileages of the tested LDDTs in our study and the variation of driving conditions for different test routes. Moreover, we suspected that the DNPH cartridge could be incapable to capture the complete HCHO emissions, as discussed above. The China IV LDDTs had similar HCHO EFs under the UDC and SSC conditions (25.5 ± 16.7 and 33.5 ± 15.7 mg/km, respectively). The HCHO EF for China IV LDDTs derived from RDE tests was 10.6 ± 14.2 mg/km, which was substantially lower than those tested by the dynamometer. However, the China V LDDTs performed differently. The HCHO EFs measured by UDC tests and RDE tests were similar, with values of 7.4 ± 4.3 and 8.8 ± 5.1 mg/km, respectively. The HCHO EF tested under SSC was much higher, with a value of 27.5 ± 14.1 mg/km. The China VI LDDT showed a noticeable decline in HCHO emissions with an EF of 3.2 ± 1.2 mg/km in the RDE test.

It is worth mentioning that the HCHO emissions from LDDT exhausts were 20−90 times higher than those from LDGVs (Figure S9), although the HCHO EFs decreased as the emission standards tightened. Previous studies mainly focused on HCHO emissions from light-duty passenger cars, presenting a range from 0.002 to 4.4 mg/km for China I−VI and Euro I−VI light-duty gasoline passenger cars[15,37−43] and 0.006−8.4 mg/km for China II−VI and Euro II−VI light-duty diesel passenger cars.[15,40,44−47] In contrast, even the hot-running HCHO emissions from LDDTs could be several orders of magnitude higher than the HCHO emissions from passenger cars, suggesting that more comprehensive study of LDDTs should be carried out in order to reduce their HCHO emissions.

3.5. Implications. Although the DNPH-HPLC method is widely used for sampling HCHO emissions from vehicles due to its low cost and simple operation, our comparison experiments demonstrated that the DNPH-HPLC method might underestimate HCHO emissions from LDDTs due to the sampling efficiency. In addition, the DNPH-HPLC method cannot provide high time-resolution data of HCHO emissions to understand the emission characteristics of LDDTs associated with different operating conditions. Therefore, it is important to use portable online techniques such as the PEMS-HCHO to overcome the limitations in sampling, pretreatment, and measurement so as to better understand the real-time HCHO emission characteristics of LDDTs.

The second-by-second HCHO emission patterns underlined the significant impacts of start modes and driving conditions on HCHO emissions from LDDTs. LDDT cold starts induced extremely high HCHO emissions. There was a 2−4 times difference in the HCHO EFs under various driving conditions. Moreover, the relationships between HCHO emission and speeds/accelerations were quite different, indicating that dynamometer tests cannot reflect real-world dynamic HCHO emissions. During real-world driving conditions, many factors such as driving style and traffic congestion can affect the vehicle operating conditions and exhaust emissions. As shown in Figure S18, the uncertainties of vehicle speeds resulted by these factors during the RDE tests were up to 25%, which can lead to considerable HCHO emission variations as discussed above. These results suggest that more work is needed to measure HCHO emission from RDE tests in order to fully uncover the dynamic relationships between HCHO emissions and driving style and traffic conditions, for different vehicle types.

Our findings demonstrated the high HCHO emissions from LDDTs, which could be thousands of times greater than those from passenger cars. Notably, the HCHO emissions during hot running conditions of most LDDTs tested in this study were significantly higher than the least stringent California LEV I emission standard for light-duty trucks (LDTs, 14.3 mg/km) implemented over 20 years ago, as shown in Figure 4. Even the China VI LDDTs with the lowest HCHO EFs still exceeded the California LEV III emission standard for light-duty vehicles (LDVs, 2.5 mg/km). Recent regulations in China only considered hydrocarbons detected by flame ionization detection (FID), but FID has zero response to HCHO.[28,49] Thus, HCHO emissions from vehicles are essentially unregulated. Therefore, we suggest that HCHO should be considered a regulated pollutant in vehicle emission standards in China, especially for LDDTs. Given that LDDTs presented significant discrepancies in HCHO emissions at different start and running conditions, emission standards for HCHO should be formulated considering the variance under operating conditions.

■ ASSOCIATED CONTENT

Supporting Information

The Supporting Information is available free of charge at https://pubs.acs.org/doi/10.1021/acs.est.2c07744.

Specifications of test vehicles; field deployment; test cycles and test routes; calculations; start emission contributions; HCHO emission characteristics of LDGVs; comparisons of variation patterns under different conditions; comparison of HCHO EFs; DNPH-HPLC measurement methods; comparison between LDGVs and LDDTs; NO_x emissions from LDDTs with and without SCR; kinematic parameters and HCHO emission maps on different running phases; stability of the dilution ratio; and variations of speeds during RDE tests (PDF)

■ AUTHOR INFORMATION

Corresponding Author

Junyu Zheng − *Institute for Environmental and Climate Research, Jinan University, Guangzhou 511436, China; Sustainable Energy and Environment Thrust, Function Hub, The Hong Kong University of Science and Technology (Guangzhou), Guangzhou 510000, China;* orcid.org/0000-0002-8267-7255; Email: junyuzheng@hkust-gz.edu.cn

Authors

Manni Zhu − *Institute for Environmental and Climate Research, Jinan University, Guangzhou 511436, China*

https://doi.org/10.1021/acs.est.2c07744
Environ. Sci. Technol. 2023, 57, 1592−1599

Jiamin Ou − *Department of Sociology, Utrecht University, Utrecht 3584 CH, The Netherlands*
Songdi Liao − *Institute for Environmental and Climate Research, Jinan University, Guangzhou 511436, China*
Fei Yu − *Institute for Environmental and Climate Research, Jinan University, Guangzhou 511436, China*
Menghua Lu − *School of Petroleum Engineering and Environmental Engineering, Yan'an University, Yan'an 716000, China*
Qinge Sha − *Institute for Environmental and Climate Research, Jinan University, Guangzhou 511436, China*
Junwen Liu − *Institute for Environmental and Climate Research, Jinan University, Guangzhou 511436, China*
Hancheng Zhong − *Institute for Environmental and Climate Research, Jinan University, Guangzhou 511436, China*
Zeyan Wu − *Institute for Environmental and Climate Research, Jinan University, Guangzhou 511436, China*
Zhuangmin Zhong − *Guangdong Ecological Environmental Monitoring Center, Guangzhou 510308, China*

Complete contact information is available at: https://pubs.acs.org/10.1021/acs.est.2c07744

Notes

The authors declare no competing financial interest.

■ ACKNOWLEDGMENTS

This study was supported by the National Natural Science Foundation of China (41627809 and 42205097) and the Fundamental Research Funds for the Central Universities (21622320).

■ REFERENCES

(1) Mellouki, A.; Wallington, T. J.; Chen, J. Atmospheric Chemistry of Oxygenated Volatile Organic Compounds: Impacts on Air Quality and Climate. *Chem. Rev.* **2015**, *115*, 3984−4014.
(2) Moch, J. M.; Dovrou, E.; Mickley, L. J.; Keutsch, F. N.; Cheng, Y.; Jacob, D. J.; Jiang, J.; Li, M.; Munger, J. W.; Qiao, X.; Zhang, Q. Contribution of Hydroxymethane Sulfonate to Ambient Particulate Matter: A Potential Explanation for High Particulate Sulfur During Severe Winter Haze in Beijing. *Geophys. Res. Lett.* **2018**, *45*, 11969−11979.
(3) de Gouw, J. A.; Gilman, J. B.; Kim, S.-W.; Alvarez, S. L.; Dusanter, S.; Graus, M.; Griffith, S. M.; Isaacman-VanWertz, G.; Kuster, W. C.; Lefer, B. L.; Lerner, B. M.; McDonald, B. C.; Rappenglück, B.; Roberts, J. M.; Stevens, P. S.; Stutz, J.; Thalman, R.; Veres, P. R.; Volkamer, R.; Warneke, C.; Washenfelder, R. A.; Young, C. J. Chemistry of Volatile Organic Compounds in the Los Angeles Basin: Formation of Oxygenated Compounds and Determination of Emission Ratios. *J. Geophys. Res.: Atmos.* **2018**, *123*, 2298−2319.
(4) Scheffe, R. D.; Strum, M.; Phillips, S. B.; Thurman, J.; Eyth, A.; Fudge, S.; Morris, M.; Palma, T.; Cook, R. Hybrid Modeling Approach to Estimate Exposures of Hazardous Air Pollutants (HAPs) for the National Air Toxics Assessment (NATA). *Environ. Sci. Technol.* **2016**, *50*, 12356−12364.
(5) Wang, C.; Huang, X.-F.; Han, Y.; Zhu, B.; He, L.-Y. Sources and Potential Photochemical Roles of Formaldehyde in an Urban Atmosphere in South China. *J. Geophys. Res.: Atmos.* **2017**, *122*, 11934−11947.
(6) Su, W.; Liu, C.; Hu, Q.; Zhao, S.; Sun, Y.; Wang, W.; Zhu, Y.; Liu, J.; Kim, J. Primary and Secondary Sources of Ambient Formaldehyde in the Yangtze River Delta Based on Ozone Mapping and Profiler Suite (OMPS) Observations. *Atmos. Chem. Phys.* **2019**, *19*, 6717−6736.
(7) De Smedt, I.; Müller, J.-F.; Stavrakou, T.; van der A, R.; Eskes, H.; Van Roozendael, M. Twelve Years of Global Observations of Formaldehyde in the Troposphere Using GOME and SCIAMACHY Sensors. *Atmos. Chem. Phys.* **2008**, *8*, 4947−4963.
(8) Ling, Z. H.; Zhao, J.; Fan, S. J.; Wang, X. M. Sources of Formaldehyde and Their Contributions to Photochemical O3 Formation at an Urban Site in the Pearl River Delta, Southern China. *Chemosphere* **2017**, *168*, 1293−1301.
(9) Lei, W.; Zavala, M.; de Foy, B.; Volkamer, R.; Molina, M. J.; Molina, L. T. Impact of Primary Formaldehyde on Air Pollution in the Mexico City Metropolitan Area. *Atmos. Chem. Phys.* **2009**, *9*, 2607−2618.
(10) Kaiser, J.; Wolfe, G. M.; Bohn, B.; Broch, S.; Fuchs, H.; Ganzeveld, L. N.; Gomm, S.; Häseler, R.; Hofzumahaus, A.; Holland, F.; Jäger, J.; Li, X.; Lohse, I.; Lu, K.; Prévôt, A. S. H.; Rohrer, F.; Wegener, R.; Wolf, R.; Mentel, T. F.; Kiendler-Scharr, A.; Wahner, A.; Keutsch, F. N. Evidence for an Unidentified Non-Photochemical Ground-Level Source of Formaldehyde in the Po Valley with Potential Implications for Ozone Production. *Atmos. Chem. Phys.* **2015**, *15*, 1289−1298.
(11) Wang, M.; Shao, M.; Chen, W.; Yuan, B.; Lu, S.; Zhang, Q.; Zeng, L.; Wang, Q. A Temporally and Spatially Resolved Validation of Emission Inventories by Measurements of Ambient Volatile Organic Compounds in Beijing, China. *Atmos. Chem. Phys.* **2014**, *14*, 5871−5891.
(12) Zavala, M.; Herndon, S. C.; Wood, E. C.; Onasch, T. B.; Knighton, W. B.; Marr, L. C.; Kolb, C. E.; Molina, L. T. Evaluation of Mobile Emissions Contributions to Mexico City's Emissions Inventory Using on-Road and Cross-Road Emission Measurements and Ambient Data. *Atmos. Chem. Phys.* **2009**, *9*, 6305−6317.
(13) Wu, R.; Xie, S. Spatial Distribution of Ozone Formation in China Derived from Emissions of Speciated Volatile Organic Compounds. *Environ. Sci. Technol.* **2017**, *51*, 2574−2583.
(14) Zeng, P.; Lyu, X.; Guo, H.; Cheng, H.; Wang, Z.; Liu, X.; Zhang, W. Spatial Variation of Sources and Photochemistry of Formaldehyde in Wuhan, Central China. *Atmos. Environ.* **2019**, *214*, 116826.
(15) Martinet, S.; Liu, Y.; Louis, C.; Tassel, P.; Perret, P.; Chaumond, A.; André, M. Euro 6 Unregulated Pollutant Characterization and Statistical Analysis of After-Treatment Device and Driving-Condition Impact on Recent Passenger-Car Emissions. *Environ. Sci. Technol.* **2017**, *51*, 5847−5855.
(16) George, I. J.; Hays, M. D.; Herrington, J. S.; Preston, W.; Snow, R.; Faircloth, J.; George, B. J.; Long, T.; Baldauf, R. W. Effects of Cold Temperature and Ethanol Content on VOC Emissions from Light-Duty Gasoline Vehicles. *Environ. Sci. Technol.* **2015**, *49*, 13067−13074.
(17) Karavalakis, G.; Short, D.; Vu, D.; Russell, R.; Hajbabaei, M.; Asa-Awuku, A.; Durbin, T. D. Evaluating the Effects of Aromatics Content in Gasoline on Gaseous and Particulate Matter Emissions from SI-PFI and SIDI Vehicles. *Environ. Sci. Technol.* **2015**, *49*, 7021−7031.
(18) Ban-Weiss, G. A.; McLaughlin, J. P.; Harley, R. A.; Kean, A. J.; Grosjean, E.; Grosjean, D. Carbonyl and Nitrogen Dioxide Emissions From Gasoline- and Diesel-Powered Motor Vehicles. *Environ. Sci. Technol.* **2008**, *42*, 3944−3950.
(19) Yao, Z.; Shen, X.; Ye, Y.; Cao, X.; Jiang, X.; Zhang, Y.; He, K. On-Road Emission Characteristics of VOCs from Diesel Trucks in Beijing, China. *Atmos. Environ.* **2015**, *103*, 87−93.
(20) Dong, D.; Shao, M.; Li, Y.; Lu, S.; Wang, Y.; Ji, Z.; Tang, D. Carbonyl Emissions from Heavy-Duty Diesel Vehicle Exhaust in China and the Contribution to Ozone Formation Potential. *J. Environ. Sci.* **2014**, *26*, 122−128.
(21) Karavalakis, G.; Gysel, N.; Schmitz, D. A.; Cho, A. K.; Sioutas, C.; Schauer, J. J.; Cocker, D. R.; Durbin, T. D. Impact of Biodiesel on Regulated and Unregulated Emissions, and Redox and Proinflammatory Properties of PM Emitted from Heavy-Duty Vehicles. *Sci. Total Environ.* **2017**, *584*−*585*, 1230−1238.
(22) Yao, Z.; Jiang, X.; Shen, X.; Ye, Y.; Cao, X.; Zhang, Y.; He, K. On-Road Emission Characteristics of Carbonyl Compounds for Heavy-Duty Diesel Trucks. *Aerosol Air Qual. Res.* **2015**, *15*, 915−925.

(23) Williams, J.; Li, H.; Ross, A. B.; Hargreaves, S. P. Quantification of the Influence of NO2, NO and CO Gases on the Determination of Formaldehyde and Acetaldehyde Using the DNPH Method as Applied to Polluted Environments. *Atmos. Environ.* **2019**, *218*, 117019.
(24) Herrington, J. S.; Hays, M. D. Concerns Regarding 24-h Sampling for Formaldehyde, Acetaldehyde, and Acrolein Using 2,4-Dinitrophenylhydrazine (DNPH)-Coated Solid Sorbents. *Atmos. Environ.* **2012**, *55*, 179−184.
(25) Szulejko, J. E.; Kim, K. H. Derivatization Techniques for Determination of Carbonyls in Air. *TrAC, Trends Anal. Chem.* **2015**, *64*, 29−41.
(26) Stępień, Z.; Czerwinski, J. Cold Start with Ethanol-Blend Fuels and Influences on Non-Legislated Emissions of a GDI Flex Fuel Vehicle. *Pol. J. Environ. Stud.* **2017**, *26*, 2223−2229.
(27) Suarez-Bertoa, R.; Clairotte, M.; Arlitt, B.; Nakatani, S.; Hill, L.; Winkler, K.; Kaarsberg, C.; Knauf, T.; Zijlmans, R.; Boertien, H.; Astorga, C. Intercomparison of Ethanol, Formaldehyde and Acetaldehyde Measurements from a Flex-Fuel Vehicle Exhaust during the WLTC. *Fuel* **2017**, *203*, 330−340.
(28) Gierczak, C. A.; Kralik, L. L.; Mauti, A.; Harwell, A. L.; Maricq, M. M. Measuring NMHC and NMOG Emissions from Motor Vehicles via FTIR Spectroscopy. *Atmos. Environ.* **2017**, *150*, 425−433.
(29) Ko, J.; Son, J.; Myung, C. L.; Park, S. Comparative Study on Low Ambient Temperature Regulated/Unregulated Emissions Characteristics of Idling Light-Duty Diesel Vehicles at Cold Start and Hot Restart. *Fuel* **2018**, *233*, 620−631.
(30) Zhu, M.; Dong, H.; Yu, F.; Liao, S.; Xie, Y.; Liu, J.; Sha, Q.; Zhong, Z.; Zeng, L.; Zheng, J. A New Portable Instrument for Online Measurements of Formaldehyde: From Ambient to Mobile Emission Sources. *Environ. Sci. Technol. Lett.* **2020**, *7*, 292−297.
(31) Ministry of Ecology and Environment of the People's Republic of China. *China Mobile Source Environmental Management Annual Report*, 2019.
(32) Liao, S.; Zhang, J.; Yu, F.; Zhu, M.; Liu, J.; Ou, J.; Dong, H.; Sha, Q.; Zhong, Z.; Xie, Y.; Luo, H.; Zhang, L.; Zheng, J. High Gaseous Nitrous Acid (HONO) Emissions from Light-Duty Diesel Vehicles. *Environ. Sci. Technol.* **2021**, *55*, 200−208.
(33) Wen, Y.; Zhang, S.; He, L.; Yang, S.; Wu, X.; Wu, Y. Characterizing Start Emissions of Gasoline Vehicles and the Seasonal, Diurnal and Spatial Variabilities in China. *Atmos. Environ.* **2021**, *245*, 118040.
(34) Drozd, G. T.; Zhao, Y.; Saliba, G.; Frodin, B.; Maddox, C.; Weber, R. J.; Chang, M.-C. O.; Maldonado, H.; Sardar, S.; Robinson, A. L.; Goldstein, A. H. Time Resolved Measurements of Speciated Tailpipe Emissions from Motor Vehicles: Trends with Emission Control Technology, Cold Start Effects, and Speciation. *Environ. Sci. Technol.* **2016**, *50*, 13592−13599.
(35) Wei, Y.; Liu, S.; Liu, F.; Liu, J.; Zhu, Z.; Li, G. Aldehydes and Methanol Emission Mechanisms and Characteristics from a Methanol/Gasoline-Fueled Spark-Ignition (SI) Engine. *Energy Fuels* **2009**, *23*, 6222−6230.
(36) Weilenmann, M.; Favez, J. Y.; Alvarez, R. Cold-Start Emissions of Modern Passenger Cars at Different Low Ambient Temperatures and Their Evolution over Vehicle Legislation Categories. *Atmos. Environ.* **2009**, *43*, 2419−2429.
(37) Caplain, I.; Cazier, F.; Nouali, H.; Mercier, A.; Déchaux, J.-C.; Nollet, V.; Joumard, R.; André, J.-M.; Vidon, R. Emissions of Unregulated Pollutants from European Gasoline and Diesel Passenger Cars. *Atmos. Environ.* **2006**, *40*, 5954−5966.
(38) Zhao, H.; Ge, Y.; Hao, C.; Han, X.; Fu, M.; Yu, L.; Shah, A. N. Carbonyl Compound Emissions from Passenger Cars Fueled with Methanol/Gasoline Blends. *Sci. Total Environ.* **2010**, *408*, 3607−3613.
(39) Zhao, H.; Ge, Y.; Tan, J.; Yin, H.; Guo, J.; Zhao, W.; Dai, P. Effects of Different Mixing Ratios on Emissions from Passenger Cars Fueled with Methanol/Gasoline Blends. *J. Environ. Sci.* **2011**, *23*, 1831−1838.
(40) Louis, C.; Liu, Y.; Tassel, P.; Perret, P.; Chaumond, A.; André, M. PAH, BTEX, Carbonyl Compound, Black-Carbon, NO2 and Ultrafine Particle Dynamometer Bench Emissions for Euro 4 and Euro 5 Diesel and Gasoline Passenger Cars. *Atmos. Environ.* **2016**, *141*, 80−95.
(41) Dai, P.; Ge, Y.; Lin, Y.; Su, S.; Liang, B. Investigation on Characteristics of Exhaust and Evaporative Emissions from Passenger Cars Fueled with Gasoline/Methanol Blends. *Fuel* **2013**, *113*, 10−16.
(42) Wang, X.; Ge, Y.; Liu, L.; Peng, Z.; Hao, L.; Yin, H.; Ding, Y.; Wang, J. Evaluation on Toxic Reduction and Fuel Economy of a Gasoline Direct Injection- (GDI-) Powered Passenger Car Fueled with Methanol−Gasoline Blends with Various Substitution Ratios. *Appl. Energy* **2015**, *157*, 134−143.
(43) Cao, X.; Yao, Z.; Shen, X.; Ye, Y.; Jiang, X. On-Road Emission Characteristics of VOCs from Light-Duty Gasoline Vehicles in Beijing, China. *Atmos. Environ.* **2016**, *124*, 146−155.
(44) Karavalakis, G.; Stournas, S.; Bakeas, E. Light Vehicle Regulated and Unregulated Emissions from Different Biodiesels. *Sci. Total Environ.* **2009**, *407*, 3338−3346.
(45) Zervas, E. Regulated and Non-Regulated Pollutants Emitted from Two Aliphatic and a Commercial Diesel Fuel. *Fuel* **2008**, *87*, 1141−1147.
(46) Karavalakis, G.; Bakeas, E.; Stournas, S. Influence of Oxidized Biodiesel Blends on Regulated and Unregulated Emissions from a Diesel Passenger Car. *Environ. Sci. Technol.* **2010**, *44*, 5306−5312.
(47) Karavalakis, G.; Boutsika, V.; Stournas, S.; Bakeas, E. Biodiesel Emissions Profile in Modern Diesel Vehicles. Part 2: Effect of Biodiesel Origin on Carbonyl, PAH, Nitro-PAH and Oxy-PAH Emissions. *Sci. Total Environ.* **2011**, *409*, 738−747.
(48) United States Environmental Protection Agency (USEPA). *Federal and California Light-Duty Vehicle Emissions Standards for Air Pollutants*, 2019.
(49) Dojahn, J. G.; Wentworth, W. E.; Stearns, S. D. Characterization of Formaldehyde by Gas Chromatography Using Multiple Pulsed-Discharge Photoionization Detectors and a Flame Ionization Detector. *J. Chromatogr. Sci.* **2001**, *39*, 54−58.

https://doi.org/10.1021/acs.est.2c07744
Environ. Sci. Technol. 2023, 57, 1592−1599